Nuclear Engineering and Technology 55 (2023) 2678–2686

Contents lists available at ScienceDirect

Nuclear Engineering and Technology

journal homepage: www.elsevier.com/locate/net

Original Article

Neutronic and thermohydraulic blanket analysis for hybrid fusion–fission reactor during operation

Sergey V. Bedenko [a,*], Igor O. Lutsik [a], Vadim V. Prikhodko [b], Anton A. Matyushin [c], Sergey D. Polozkov [a], Vladimir M. Shmakov [d], Dmitry G. Modestov [d], Hector Rene Vega–Carrillo [e]

[a] Tomsk Polytechnic University, 634050, Tomsk, Russian Federation
[b] Budker Institute of Nuclear Physics of Siberian Branch Russian Academy of Sciences, 630090, Novosibirsk, Russian Federation
[c] Joint Stock Company OKB Gidropress, 142103, Podolsk, Russian Federation
[d] Federal State Unitary Enterprise “Russian Federal Nuclear Center–Zababakhin All–Russia Research Institute of Technical Physics”, 456770, Russian Federation
[e] Academic Unit of Nuclear Studies of the Autonomous University of Zacatecas, C. Cipres 10, Fracc. La Peñuela, 98068, Zacatecas Zac., Mexico

ARTICLE INFO

Article history:
Received 17 September 2022
Received in revised form
3 March 2023
Accepted 26 March 2023
Available online 30 March 2023

Keywords:
Hybrid fusion–fission reactor facility
Thorium
D–T neutrons
Neutronic and thermohydraulic studies

ABSTRACT

This work demonstrates the results of full-scale numerical experiments of a hybrid thorium-containing fuel plant operating in a state close to critical due to a controlled source of D–T neutrons. The proposed facility represented a level of generated power (~10–100 MW_t) in a small pilot. In this work, the simulation of the D–T neutron plasma source operation in conjunction with the facility blanket was performed. The fission of fuel nuclei and the formation of spatial-energy release were studied in this simulation, in pulsed and stationary modes of the facility operation. The optimization results of neutronic and fluid dynamics studies to level the emerging offsets of the radial energy formed in the volume of the facility multiplying part due to the pulsed operation of the D–T neutron plasma source were presented. The results will be useful in improving the power control-based subcriticality monitoring method in coupled systems of the “pulsed neutron source–subcritical fuel assembly” type.

1. Introduction

The current state of research in nuclear and thermonuclear energy, and building power plant areas necessitates the further development of nuclear energy as a hybrid system [1–21]. With this aim, in February 2022, at the open scientific seminar Controlled Fusion and Plasma Technologies, State Corporation Rosatom, announced innovative nuclear systems using tokamak-based sources of thermonuclear neutrons [10].

One example of such facilities is a detailed project for the tokamak with reactor technologies designed in Russia [10], in which a blanket with nuclear fuel covers thermonuclear plasma torus. The facility includes one subsystem containing ^2H and ^3H isotopes for the fusion process and another that represents a blanket loaded with isotopic composition fuel characteristic of typical fission reactors. Korea Superconducting Tokamak Advanced Research (KSTAR) is another similar facility developed in Korea Institute of Fusion Energy (https://www.kfe.re.kr/eng/index) where a 30-s plasma confinement at 100 million °C (on November 2021 [20]) has been achieved. The second one is The Experimental Advanced Superconducting Tokamak (EAST) (on January 2022 [21]) which belongs to Institute of Plasma Physics Chinese Academy Of Sciences (http://english.ipp.cas.cn). This facility kept the 70 million °C heated plasma for 1056 s.

Another project of a hybrid reactor is a volume loaded with fuel for nuclear fission reactors receiving additional neutrons from outside that are produced in (p, n) reactions [1,2,15,16,21]. Implementing such a hybrid power plant with external neutron fluxes emerging from the tokamak plasma or from a target irradiated by the proton beam from a high energy accelerator is acceptable for

Abbreviations: HGTRU, High-temperature gas-cooled thorium reactor unit; PSN, Plasma source neutron; HTGR, High-temperature gas-cooled reactor; HTTR, High-temperature engineering test reactor; PCSM, power control-based subcriticality monitoring; WG, Weapons-grade; IAEA, International Atomic Energy Agency.

* Corresponding author. School of Nuclear Science and Engineering, National Research Tomsk Polytechnic University, 634050, Tomsk, Russian Federation.
E-mail address: bedenko@tpu.ru (S.V. Bedenko).

https://doi.org/10.1016/j.net.2023.03.032
1738-5733/

practice only with its tens of Gigawatts of power. This power level determines the possibility of such a power station in the distant future [3,5]. On the other hand, nuclear power plants with less power can be designed, which will be more reliable in the near future. This work aims to develop the facility for a power level of about 60 MW_t using the positive features of hybrid power plants. Creating a pilot facility with mentioned moderate power level is possible in the next 15–20 years. In this case, it opens up the possibility for practice application of the energy hybrid power plants in an acceptable, relatively short time. Therefore, it has been decided to study the development of small types to have the prospect of entering the field of using energy in the near future [7–9,13,17].

The facility modeled in the present study is a hybrid reactor with a core (i.e., blanket) consisting of prismatic graphite-block assemblies and an additional extended plasma source of D–T neutrons (PSN) with a linear configuration (see Fig. 1 [9] and Table 1).

The transfer of additionally generated neutrons to the entire hybrid system working in subcritical operation mode ($k_{eff} = 0.95$, with the corresponding neutron amplification value of 20) can increase the nuclear safety level. It should be noted that safe operation will depend largely on the reliable operation of the PSN and its structural elements (i.e., the reliability of superconducting magnets, mirror coils, injectors, cooling system, etc.). One should be taken that any PSN malfunction will lead to a fast decay of plasma parameters, including the rate of thermonuclear reactions, which result in the fade-out of the neutron source in case of failure.

Earlier studies [7,17] showed that when a neutron flux with an intensity of 2.56×10^{17} $n.s^{-1}$ enters the multiplying blanket region in the PSN facility, the neutron flux will increase to ~10^{19} $n.s^{-1}$. In the repetitively pulsed mode of the PSN operation, its flux forms an offset of the energy release field and, consequently, a temperature field gradient. This requires a separate study of the temporal dynamics behavior of the fission process of fuel nuclei.

In this research, the optimization of thermophysical characteristics is presented, and the discussions are presented on the fluid dynamics modeling to level the resulting offsets of the radial and axial energy release components formed in the blanket volume due to the pulsed mode of the PSN operation.

These computational studies will make it possible to begin the creation and organization of reliable operation of a subcritical facility, which enables conducting experiments to study the properties of fuel and materials, and the possibility of their application in hybrid and thermonuclear systems. If the pilot experiments are successful, the fusion–fission plant under study can be integrated into the existing small generation fleet and the energy system of the future thermonuclear power industry.

Studies on increasing the PSN brightness and modeling its operating modes were conducted using the DOL [17] and PRIZMA [22] programs. Neutronic, thermophysical optimization and thermohydraulic calculations were carried out using verified Serpent 2.1.31 [23] and Siemens Simcenter FloEFD 2020.2 [24] software codes. The developed models and results, as well as various aspects of the solutions obtained earlier, are demonstrated and discussed in the next sections.

2. Materials and methods

This section describes the models and methods of three calculation steps. In the first step, the magnetic field was calculated using the DOL code and the optimal D–T configuration of the source and the spatial-energy distribution of neutrons were obtained. The second step analyzes the stationery and pulse–periodic operation of the PSN in conjunction with the blanket. The computational analysis was performed using the DOL and PRIZMA programs. The obtained results and data sets were used as input parameters for specifying the source D–T and calculating the energy release peak values using the Serpent 2.1.31 code. In the third step, using Siemens Simcenter FloEFD 2020.2. The cooling conditions of the blanket and PSN are studied.

2.1. Neutronic blanket model

In the proposed fusion–fission reactor, the blanket part of the facility is based on the active-zone concept of a multi-purpose high-temperature gas-cooled low-power reactor unit (HGTRU) [8,18,19] with a near-axial region modified under the PSN [13]. The modified core (see Figs. 1 and 2a and b, and Table 1) is a blanket composed of prismatic graphite fuel containing dispersive fuel in the channels and fuel-free blocks.

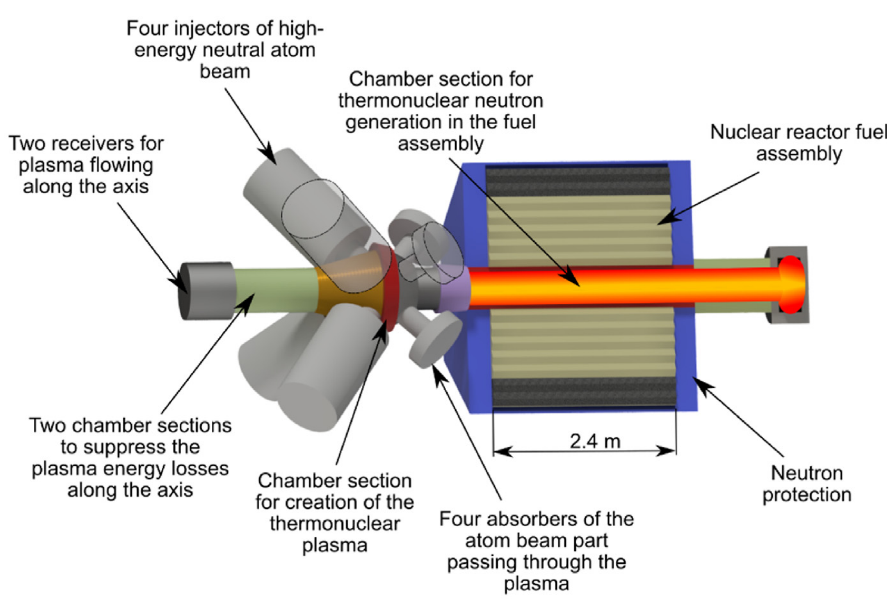

Fig. 1. The conceptual design of a hybrid fusion–fission reactor facility.

Table 1
Technical specifications of the blanket and PSN.

Specification	Value
Thermal power (MW_t)	60
Coolant pressure (MPa)	10
Blanket parameters	
Height (m)	3
Fuel section height (m)	2.4
Width (m)	2.762
Number of fuel blocks in core (pcs)	216
Mass of heavy metals (kg)	290.77
Fuel block parameters	
Width (m)	0.208
Height (m)	0.8
Number of channels for fuel (pcs)	76
Number of channels for coolant (pcs)	7
The diameter of channels for fuel (m)	10.17×10^{-3}
The diameter of channels for coolant (m)	24×10^{-3}
Fuel compact parameters	
Height (m)	20×10^{-3}
Diameter (m)	10.17×10^{-3}
SiC coating thickness (μm)	300
Volume fraction of the dispersed phase (not-profiled blanket)	0.17
Atomic fraction $^{wg}Pu/Th$ (%)	50/50
^{wg}Pu isotopes (%)	^{239}Pu (94) ^{240}Pu (5) ^{241}Pu (1)
PSN parameters	
Length of the plasma column in the neutron-producing section (m)	3
Outer diameter of the solenoid inside the subcritical assembly (m)	0.6
Inner diameter of the vacuum chamber in the neutron-producing section (m)	0.35
Magnetic field in the neutron-producing section (T)	2.0–2.5
Length of a plasma column with sloshing ions (m)	12
Magnetic field in the section for neutral beam injection (T)	0.7–1.0
Magnetic field in the mirror plug (T)	15
Particle energy of the injected beams (keV)	40
Total power of beam injection (MW)	70
Total neutron yield from plasma ($n.s^{-1}$)	5.64×10^{17}

The dispersed fuel is a homogeneous–heterogeneous structure of microscopic bistructural isotropic fuel particles encapsulated inside a graphite fuel compact (see Fig. 2b). Fuel particles include a kernel ($^{weapons\text{-}grade(wg)}Pu$ and thorium dioxides) and two layers of functional coatings–PyC and Ti_3SiC_2. Helium, traditional for this reactor type, is used as a coolant, and graphite is used as the main structural material of the blanket and moderator.

Interest in the design of the HGTRU blanket [8,18,19] is due to the following features of the core, which are also characteristic of typical HTGRs [25–29].

- High rates of inherent safety;
- Thermal stability of micro-encapsulated fuel, functional coatings, and core structural materials;
- Inert and non-activated coolant;
- The possibility of generating high-potential heat, which makes enables using a power unit of this type not only for generating electricity but also for pyrochemical processing of chemical industries.

In addition, the structural features of the encapsulated fuel enable achieving very high burn-up at enrichment of up to 20%, i.e., the border of the “HEU” category according to the IAEA classification [30] is not crossed, which, subject to IAEA safeguards, has a positive effect on both efficiency and economy facility.

The work analyzes the facility's operation with a (^{wg}Pu–^{nat}Th) O_2–blanket (see Table 1). The main reason for considering the possibility of using ^{wg}Pu [31] (^{239}Pu (47%), ^{240}Pu (2.5%), ^{241}Pu (0.5%)), and ^{nat}Th (50%) is the economic attractiveness of this composition for Russian and several other regions. Thorium has a minimal price since natural thorium consists of a single isotope and does not require complex isotope separation technology. The reserves of thorium on the planet exceed the reserves of uranium by 4–5 times. Thorium deposits are more accessible (for example, in the Siberian region in Russia, near Tomsk and Novokuznetsk) than uranium. At the same time, it is also important that thorium and plutonium have already been accumulated in large quantities in Russia and in the world.

Using additional PSN neutrons improves the inherent safety of the reactor and the possibility of irradiating special targets with neutrons with an energy of 14.1 MeV, which enables using fuel of any isotopic composition and effectively burn-up ^{wg}Pu and minor actinides.

Given these and other well-known advantages of thorium compositions [32], as well as the positive aspects of subcritical nuclear facilities, an HGTRU [8,18] with a modified para-axial region under the PSN is an attractive solution for the future energy.

2.2. Plasma-physical model of PSN

The PSN (see Fig. 2c) [13] is a plasma-extended vacuum chamber with a linear configuration (axially symmetrical plasma trap), in which the magnetic field maintains the required high-temperature plasma. This area is limited by magnetic mirrors, which are located at the coordinates $y_1 = -5$ m and $y_2 = 10$ m, as seen in Fig. 3. This area of the vacuum chamber can be conditionally divided into two parts. The first one is designed to accommodate atomic beam injectors where the magnetic field induction of the chamber is practically independent of the y-coordinate in its value range of -1.8 m $< y < 2.2$ m.

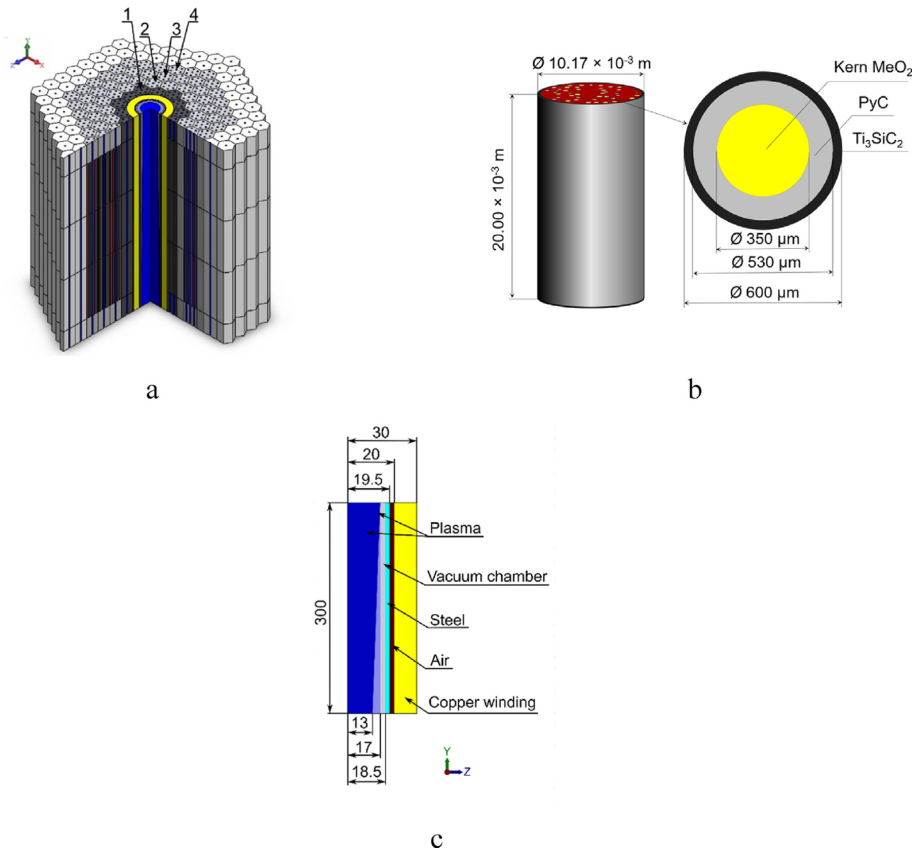

Fig. 2. The schematic view of the solution design for a hybrid fusion–fission reactor facility: (a) The 3D model of the facility (1–4 are numbers of rows with fuel and non-fuel blocks, (b) Fuel compact and micro-encapsulated fuel; (c) The PSN 3D model (dimensions are given in centimeters).

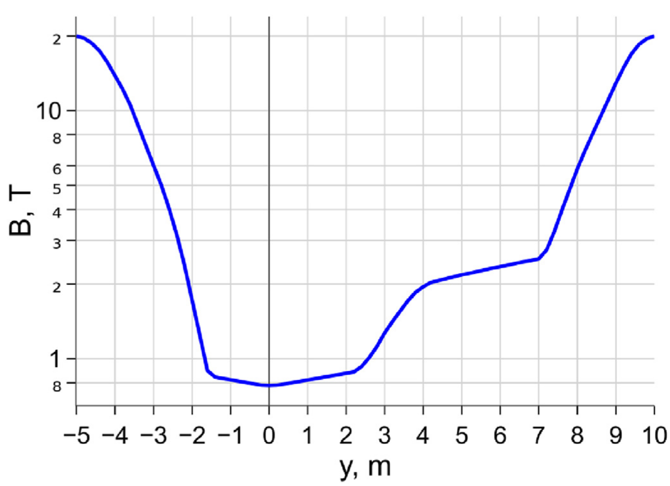

Fig. 3. Magnetic field induction B(y) as a function of the y-coordinate along the setup axis.

The second chamber part (see coordinates 4 m < y < 7 m) was located inside the subcritical blanket. The primary D–T neutrons were generated in this 3-m part of the chamber. The magnetic field was slowly built up here, providing an almost uniform neutron production profile.

The generation of thermonuclear neutrons in PSN was simulated using the computer code DOL [17]. The DOL code is based on three main components of the model. The first of them is a solver of the non-stationary Fokker–Planck kinetic equation. It can be used to simulate the dynamics of the distribution function of high energy fast sloshing ions in a magnetic trap. The second component is the solver of non-stationary particles and energy balance equations for the background plasma. This plasma includes warm ions and electrons with temperatures below 1 keV. It is assumed that this plasma has a temperature much lower than the average energy of fast sloshing ions and has a Maxwellian distribution function. The third component is the solver of the stationary kinetic equation for the neutral gas distribution function in a magnetic trap. It allows one to calculate the interaction between plasma and neutral beams, which are created by a system of injectors. These neutral beams provide heating of the plasma.

Having taken into consideration of the plasma parameters reported in Ref. [17] (the optimal design variant v5 according to Ref. [17] was obtained for a configuration with the following parameters: $P_{inj} = 30$ MW and $E_{inj} = 70$ keV), the generation process of primary D–T neutrons was performed with new initial parameters (design variant v6).

In the present work, the optimum v6 design is achieved through suppressing longitudinal losses by multiple-mirror sections at a total injection power P_{inj} of 40 MW and an energy of injected atoms E_{inj} of 70 keV (see the v6 design variant in Table 2), resulting in a total neutron yield of 5.64×10^{17} $n.s^{-1}$.

In this configuration, the radius of the plasma column in the 3-m blanket part was fixed at a distance of 10 cm. In contrast to variant v5, the shape of the D–T source was almost cylindrical.

The longitudinal profile of the neutron yield $Y_n(y)$ for the optimal variant v6 is the facility in Fig. 4. This optimal $Y_n(y)$ was used in calculations to find the energy distribution of the neutron flux density $\phi_{fusion}(E)$ (see Fig. 5) coming from the PSN to the

Table 2
Parameters of the optimal configuration of the D–T source for the calculation undertaken in v6 (the parameters for deuterium and tritium are separated by a slash).

Calculation variant	v6
Plasma isotope composition	50% D + 50% T
Plasma radius in central plane (cm)	20
Axial losses suppression provided by multimirror sections	4
Injection power (MW)	40
Injection energy (keV)	70
Gas feed rate (eq. A)	3.2/3.2
Temperature of electrons (keV)	0.77
Temperature of ions (keV)	0.72/0.70
Fast ion density in the blanket (10^{13} cm^{-3})	5.5/7.5
Warm ion density in the blanket (10^{13} cm^{-3})	1.8/2.3
Maximum relative pressure β	0.22
Captured part of injection power	0.95/0.98
Classical to gas-dynamic confinement times ratio	0.95/1.06
Neutron yield in the blanket (n.s^{-1})	2.55×10^{17}
Total neutron yield from plasma (n.s^{-1})	5.64×10^{17}

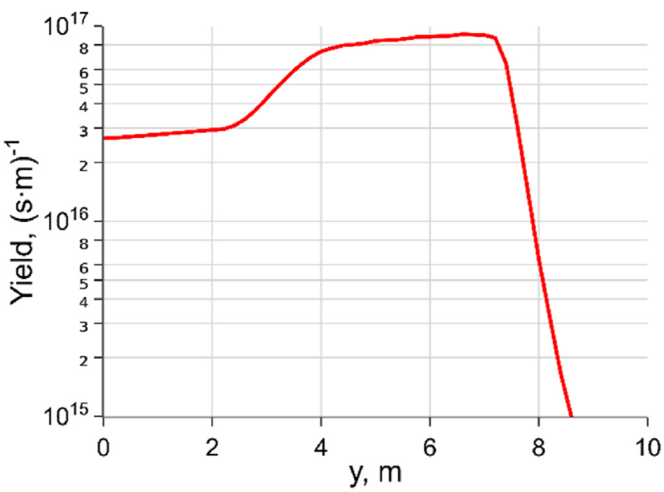

Fig. 4. The longitudinal profile of the neutron yield $Y_n(y)$ versus the distance from the plasma column.

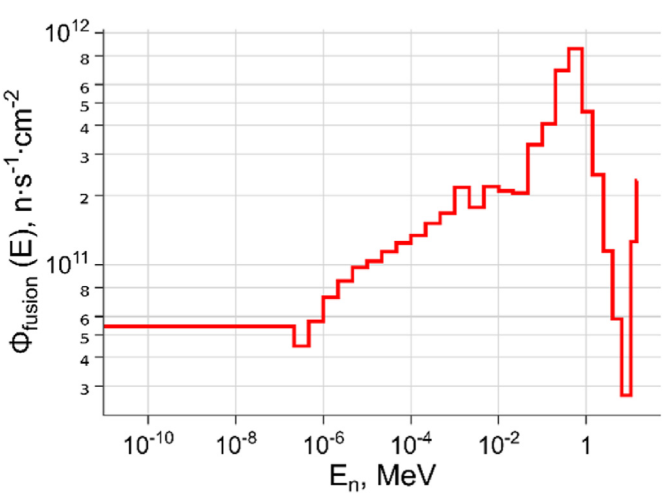

Fig. 5. Energy distribution of neutron flux density PSN.

blanket part of the facility. Spatial (see Fig. 4) and energy (see Fig. 5) distribution of neutrons were input data sets for 3D neutronic and thermophysical calculations.

It should be noted that the plasma column was formed in a repetitively pulsed regime in the PSN–blanket configuration of this study. Basically, the wave of the nuclear fissions occurs in (^{wg}Pu–$^{nat}Th)O_2$ fuel and then propagates from the axial region over the entire multiplying part in a time correlation with the operating PSN.

The simulation of the PSN operation in conjunction with the facility blanket was carried out with the PRIZMA code. However, some necessary subroutines were provided by the team in FSUE "RFNC–VNIITF named after Academ. E.I. Zababakhin" [22]. The simulation used the estimated pointwise nuclear data converted from the ENDF-B/VII.1 library [33], as well as additional data for neutron scattering in graphite from the ENDF-B/VII.0 library. In each calculation, 10^9 histories were played, ensuring the accuracy of the desired solution equal to 0.01%.

The simulation model (see Fig. 6a and b) used in simulations with the PRIZMA code involved an axially symmetric 3D configuration with four regions of different properties, which were separated by circles with radii of 30, 41.03, 89.8, and 122.4 cm.

The inner axial region of the model (yellow circle in the center in Fig. 6b) contained a pulse–periodic source of D–T neutrons, and the outer region (gray ring) contained a graphite reflector. Between these areas, a fuel blanket consisting of 50 layers of equal volume were used, which were filled with homogenized (^{wg}Pu–$^{nat}Th)O_2$ fuel (brown ring in Fig. 6b) and a layer of graphite without fuel blocks (gray ring in Fig. 6b, adjacent to D–T neutrons).

The performed calculations of the spatiotemporal parameters of PSN for various emission modes showed that when the duration of the thermonuclear combustion pulse and the duty cycle were 1 ms and 2, respectively, the observed peak in the fission rate (fission•s^{-1}•source^{-1}) in the impulse became less noticeable and almost negated. In the first layer of fuel blocks adjacent to the PSN, the influence of the pulse–periodic mode was visible (see Fig. 7a, layer 5 was included in the computational region of the second row of fuel blocks). In turn, there was no non-stationarity at the periphery of the fuel part (see Fig. 7b, layer 50 was included in the computational region of the fourth (peripheral) row of fuel blocks).

It should be noted that the asymptotic state (steady-state) was observed in the time interval from 0.1 to 1 s. In a second state, the total number of fissions in the blanket increased to 20 (per one neutron from the PSN to the blanket). This value did not change further, providing blanket heating at a constant rate. Thus, the facility must be started with a warm blanket to exclude the destructive effect of the PSN pulse mode on the fuel blocks at the startup moment.

Computational analysis of the balance of fission neutrons (see in Fig. 8 for energy $\phi_{fission}(E)$ and spatial $\phi_{fission}(R)$ distributions) generated in the blanket 1 s after the PSN startup (i.e., when the asymptote is reached) showed that their spectrum $\phi_{fission}(E)$ (see Fig. 8a) contained 28.12% neutrons with energies from 0 to 0.5 eV (blue line in Figs. 8b and 51.05% of neutrons with energies from 0.5 eV to 100 keV (green line in Figs. 8b) and 20.84% (red line in Fig. 8b) with energies from 100 keV up to 20 MeV. Thus, the (^{wg}Pu–$^{nat}Th)O_2$–blanket powered by additional D–T neutrons PSN was a fusion–fission system with an epithermal neutron spectrum, i.e., with a spectrum characteristic of breeder systems. The dependence of the neutron flux density $\phi_{fission}(R)$ on the radius (for layers from 1 to 50) for three energy groups is illustrated in Fig. 8b.

After analyzing the obtained results, it was decided to consider the pulsed neutrons as a quasi-stationary source and use a reactor simulation program code based on the Serpent 2.1.31 (JENDL-4.0) [33] Monte Carlo method for optimization purposes. In each calculation, 10^7 histories were played, making it possible to ensure the desired solution's accuracy equaled 0.1%.

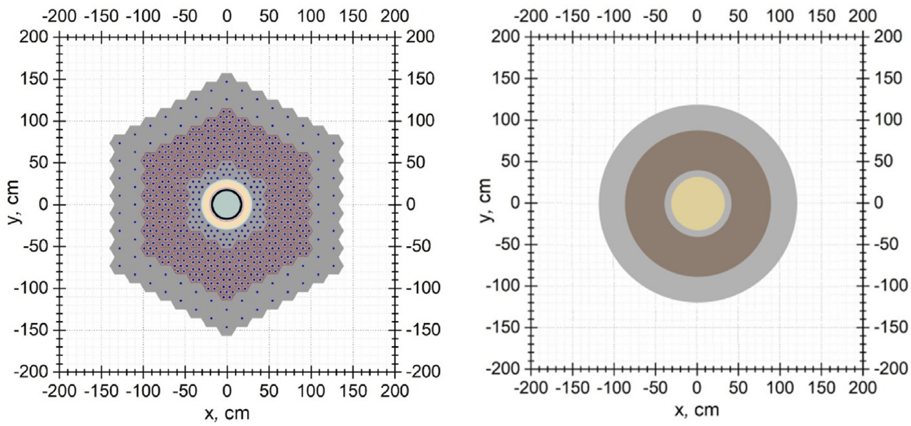

Fig. 6. (a) The cross-section of the original configuration and (b) the equivalent simulation 3D model.

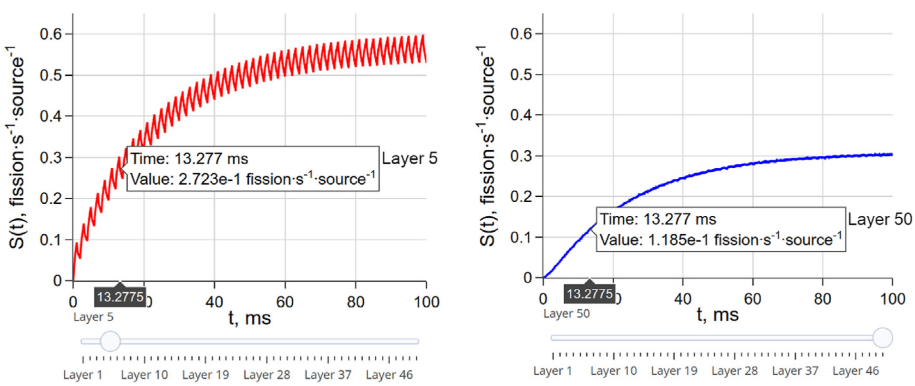

Fig. 7. The fission rate in the blanket powered by the pulse PSN. The numbers of layers indicated on the scale were the calculated areas of equal volume in which the blanket part of the facility was divided, to display more accurate data on the fission rate in the fuel elements 2–4 (see specifiers in Fig. 2a).

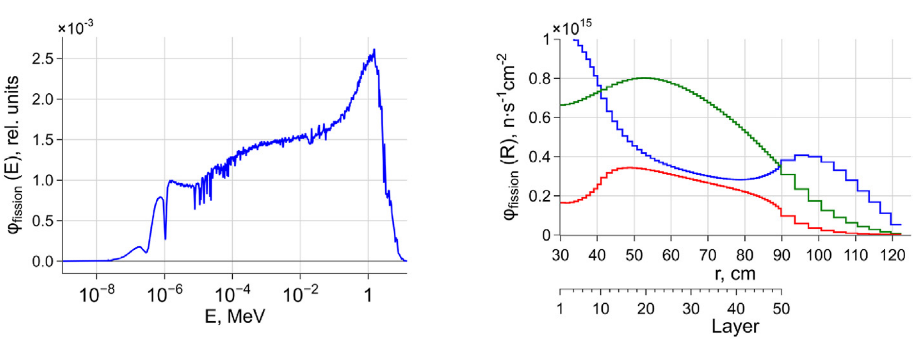

Fig. 8. (a) Energy and (b) spatial neutron flux density distribution in the facility blanket.

2.3. Thermohydraulic blanket model

Thermohydraulic modeling was performed by the finite element method in the conjugate formulation: both heat transfer due to heat conduction and convective heat transfer were considered. The blanket configuration is shown in Fig. 2a. We used the standard FloEFD mesh generator from the Siemens Simcenter FloEFD 2020.2 program code [24] to construct the mesh model. According to the optimization results in the previous step, the energy release was assumed to be the same in all fuel blocks. For the 1/12 blanket model, the thermal power in the calculations was assumed to be 5000 kW_t.

A series of optimization parametric calculations were carried out for effective cooling of the blanket and PSN. In the calculations, the coolant parameters (temperature, pressure, and velocity) were the variable parameters, and the target ones were the temperature extremes of the PSN materials and the blanket. The thermophysical properties of helium, structural materials and fuel, and the built-in FloEFD library and research results [34] were used to choose the helium parameters. The calculation results for the main operating parameters (fuel and graphite temperatures; coolant temperature, pressure, and helium velocity) of the blanket were compared with similar experimental and calculated parameters of the HTTR reference facility [25–27].

3. Results and discussion

This section presents the results of conjugate neutronic, thermophysical, and thermohydraulic calculations. This aims to determine the temperature mode for blanket cooling by a helium flow, construct temperature fields, search for temperature extremes, and estimate offsets of the energy release field in the blanket volume.

3.1. Results of neutronic and thermophysical simulation

Thermophysical optimization (see Fig. 9a and b) of the blanket was performed according to the energy release profile along the radius by changing the Pu fraction content. Fuel blocks of rows 2–4 (see specifiers 1–4 in Fig. 2a) were loaded with fuel where the volume fractions of the dispersed phase were ω_{pf} = 7%, 9%, 13%, 17%, 21%, and 31%.

Considering the loading shown in Fig. 9b, the uniformity of the radial power release profile was improved, and the power output peaks were reduced by 19% compared to the unshaped blanket part (see Fig. 9a) and by 7% compared with the results obtained earlier in Ref. [9].

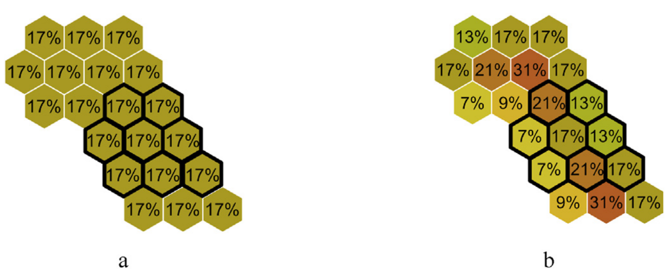

Fig. 9. (a) Cartogram of loading of non-profiled and (b) profiled multiplying part (rows 2–4) of the facility blanket.

3.2. Results of thermohydraulic simulation

The thermohydraulic simulation results (see Fig. 10) for the left 1/12th part of the sector used in the calculation model) confirmed that the temperature of both the first fuel-free and the second row of the fuel blocks were reduced to the values required for the normal PSN operation. The most energy-intensive region of the blanket was located in the third row at the height of 2.64 m. Here, the maximum fuel and graphite temperature reached 1335 °C, which did not change significantly in the azimuthal direction. In addition, an almost uniform temperature profile was found for the third and fourth rows of blocks (see Fig. 10b).

Fig. 11 shows the temperature fields on the surface of channels with coolant. Here, the maximum temperature of helium will reach 987.80 °C. At the blanket outlet (i.e., at the level of 2.7 m, see the 2700 Solid Max/Fluid level in Fig. 11), the average helium temperature of the third row with the maximum temperature load was

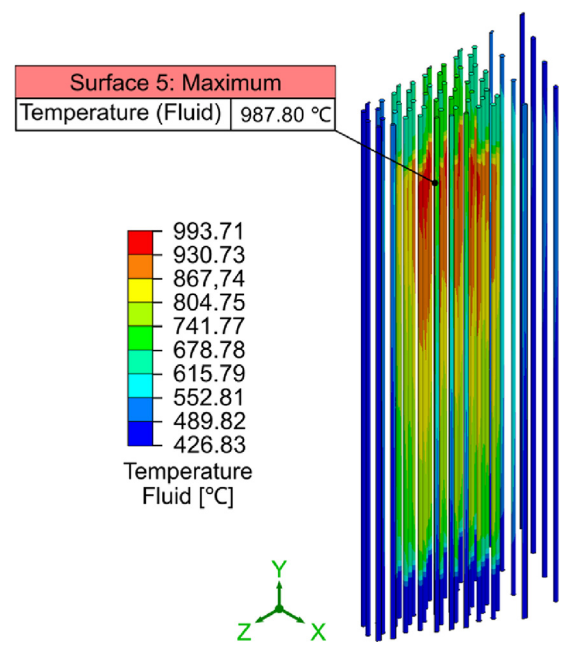

Fig. 11. The temperature field on the surface of coolant channels for the 1/12 blanket model.

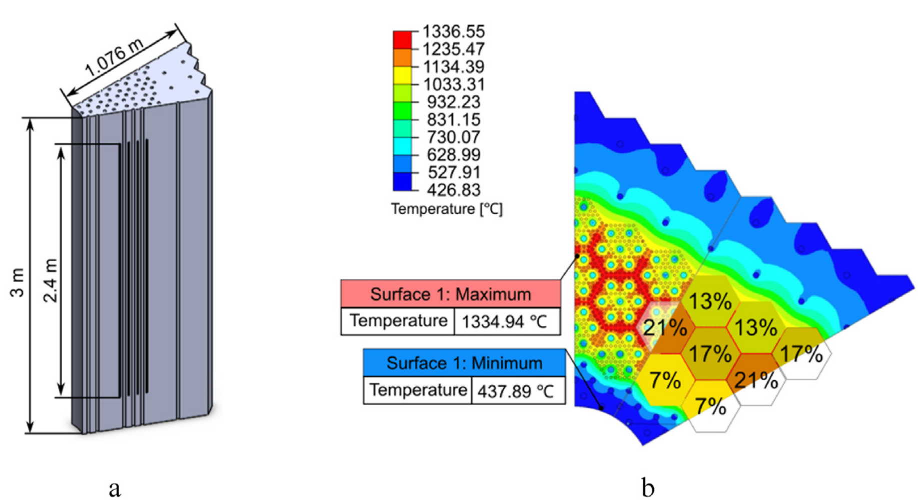

Fig. 10. (a) The model 1/12 blanket and (b) cartogram (1/6 blanket) of the load and the blanket temperature profile in the cross-section with the maximum temperature.

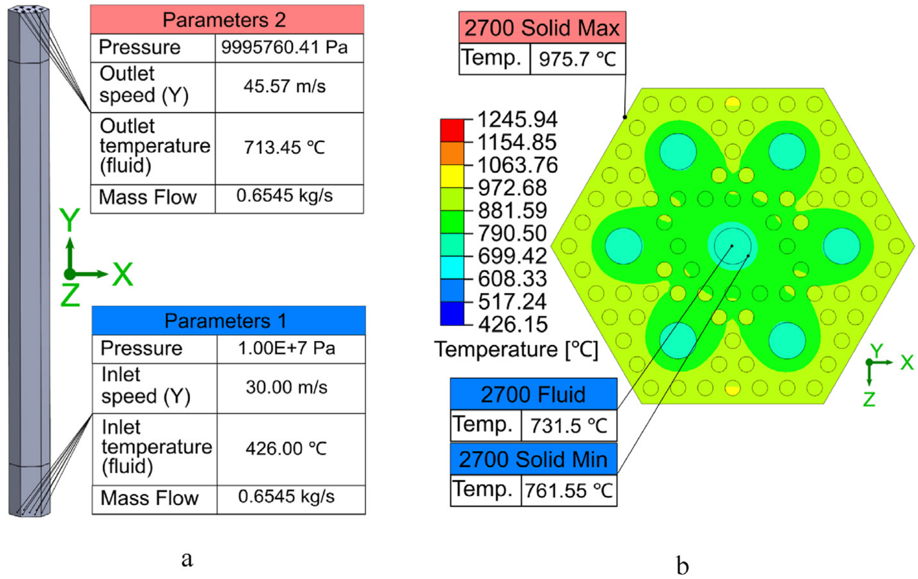

Fig. 12. (a) The column model of the third row (1/72 blanket) and (b) the temperature field of materials in the cross-section at the height of 2.7 m.

731.5 °C (see Fig. 12b, 2700 Fluid). This result was obtained for the model shown in Fig. 12a, and the boundary conditions given in Table 3.

Thus, considering an additional option allowing using the produced high-temperature heat to produce hydrogen by the steam reforming method, blanket cooling conditions were studied.

It should be noted that the operating temperatures of dispersed ($^{wg}Pu-^{nat}Th)O_2$–fuel and the graphite should not exceed 1250 °C and 1300 °C, respectively [25,29,35]. However, Fig. 10 shows that the allowable limits for fuel and graphite exceeded 6.3% and 2.6%, respectively. The boundary conditions (see Table 3) selected based on the results of a series of variant simulations, with the observed local excess of permissible limits, enabled obtaining the helium temperature required for pyrochemical stages of chemical production.

The obtained results showed satisfactory agreement between the main operational parameters (fuel and graphite temperature; coolant temperature, pressure, and helium velocity) of the setup blanket with similar experimental and calculated parameters of the reference HTTR [25–27], and other types of $HTGR_S$ [25,29,35].

The intensity of the local energy generated from the third row can be reduced, for example, by changing the flow area configuration of the channels for helium, while using the same flow area for the first, second, and fourth rows of the blocks. Using local resistance, for example, the so-called flow-measuring washers or heat transfer intensifiers, is another option that does not require a new set of neutronics and thermophysical calculations.

Generating electricity for decentralized regions is the main goal of the project. However, ongoing research may enable its use in many other applications, such as water desalination and hydrogen production, nuclear fuel breeding, and radioactive waste decontamination. Thus, if successful, integrating such a plant into the fleet of existing reactors will allow the energy of the future to become more sustainable and, in a sense, renewable.

Table 3
The main thermohydraulic parameters of the blanket.

Parameter	Value
Thermal power 1/12 of the blanket model (kW)	5000
Thermal power 1/72 of the blanket model (kW)	833.33
Pressure (Pa)	1.00E + 7
Inlet temperature (°C)	426.00
Outlet temperature (°C)	713.45
Inlet speed ($m.s^{-1}$)	30.00
Outlet speed ($m.s^{-1}$)	45.57
Mass flow ($kg.s^{-1}$)	0.6545

4. Conclusions

In the present study the operation simulation of the PSN in conjunction with the facility blanket was performed. The data sets obtained from modeling were used to study the stationary and pulse-periodic operation of the PSN. During the simulation, the fission processes of fuel nuclei and the formation of spatial-energy release were studied both in pulsed and stationary operation modes of the facility. The obtained results enabled considering the pulsed source as a quasi-stationary source and performing thermophysical optimization in neutronic studies using the Serpent code. The obtained data showed that reducing the resulting offsets of the radial field of energy release in the volume of the multiplying part of the facility was possible.

A series of optimization fluid dynamics calculations were carried out for efficient blanket and PSN cooling, in which the coolant parameters were the variable parameters, and the temperature extremes of the PSN and blanket materials were the target ones. Blanket cooling studies were done with an additional option that allowed using the produced high-temperature heat to produce hydrogen.

The research results enabled proceeding to the preliminary safe design of a subcritical pilot plant for experimental research of an applied and fundamental nature. This will help to better study the fusion process and the operation of various reactor elements under hard neutron irradiation conditions, which would significantly accelerate the development of thermonuclear energy. The results will also help improve the criticality control methods in coupled systems of the “pulsed neutron source–subcritical fuel assembly” type.

Further work is related to developing a procedure for online monitoring of the subcriticality level of the facility under study using the power control-based subcriticality monitoring method.

Research is also underway to develop a model for improved plasma production and confinement to maximize the fusion neutrons yield. In the course of these works, the multimirror section parameters to suppress the longitudinal plasma losses through magnetic mirrors will be determined. In future projects, particular attention will be given to justifying the effectiveness and safety of technical solutions for radiation protection against PSN-generated neutrons.

Declaration of competing interest

The authors declare that they have no known competing financial interests or personal relationships that could have appeared to influence the work reported in this paper.

Acknowledgments

This research was supported by the Russian Science Foundation under RSF grant No. 23-29-00131 (https://rscf.ru/en/project/23-29-00131/).

The authors are also grateful to the center of TPU's "Physical and chemical methods of analysis".

The authors are very grateful to the peer reviewers, whose comments allowed to improve the quality of the paper significantly.

References

[1] MYRRHA. [online]. The Belgian nuclear center SCK-CEN provided information on a course of construction the new isotope MYRRHA reactor https://www.sckcen.be/en/our-scientific-projects/myrrha(accessed July 27, 2022).

[2] H.A. Abderrahim, P. Kupschus, E. Malambu, P. Benoit, K. Van Tichelen, B. Arien, F. Vermeersch, P. D'hondt, Y. Jongen, S. Ternier, D. Vandeplassche, MYRRHA: a multipurpose accelerator driven system for research & development, Nucl. Instrum. Methods Phys. Res. Sect. A Accel. Spectrom. Detect. Assoc. Equip. 463 (3) (2001) 487–494.

[3] T. Donné, W. Morris, X. Litaudon, C. Hidalgo, D. McDonald, H. Zohm, P. Helander, European Research Roadmap to the Realization of Fusion Energy, 2018. https://www.euro-fusion.org/fileadmin/user_upload/EUROfusion/Documents/TopLevelRoadmap.pdf. (Accessed 8 August 2022).

[4] Z. Chen, P.A. Bagryansky, Q. Zeng, J. Zou, K. Zhang, Z. Wang, J. Jia, S. Zhang, L. Dong, X. Zha, Summary of the 3rd international workshop on gas-dynamic trap based fusion neutron source (GDT-FNS), Nucl. Fusion 62 (2) (2022), 067001.

[5] S. Entler, J.M. Horáček, T. Dlouhý, V. Dostál, Approximation of the economy of fusion energy, Energy 152 (2018) 489–497.

[6] S.S. Ananyev, B.V. Ivanov, B.V. Kuteev, Analysis of promising technologies of DEMO-FNS fuel cycle, Fusion Eng. Des. 161 (2020), 111940.

[7] A.V. Arzhannikov, V.M. Shmakov, D.G. Modestov, S.V. Bedenko, V.V. Prikhodko, I.O. Lutsik, I.V. Shamanin, Facility to study neutronic properties of a hybrid thorium reactor with a source of thermonuclear neutrons based on a magnetic trap, Nucl. Eng. Technol. 52 (11) (2020) 2460–2470.

[8] A. Arzhannikov, S. Bedenko, V. Shmakov, V. Knyshev, I. Lutsik, V. Prikhodko, I. Shamanin, Gas-cooled thorium reactor at various fuel loadings and its modification by a plasma source of extra neutrons, Nucl. Sci. Tech. 30 (12) (2019) 1–11.

[9] S.V. Bedenko, A.V. Arzhannikov, I.O. Lutsik, V.V. Prikhodko, V.M. Shmakov, D.G. Modestov, A.G. Karengin, I.V. Shamanin, Maintaining the close-to-critical state of thorium fuel core of hybrid reactor operated under control by DT fusion neutron flux, Nucl. Eng. Technol. 53 (6) (2021) 1736–1746.

[10] A.V. Krasilnikov, S. Konovalov, E.N. Bondarchuk, I.V. Mazul, I.Yu Rodin, A.B. Mineev, E.G. Kuzmin, A.A. Kavin, D.A. Karpov, V.M. Leonov, R.R. Khairutdinov, A.S. Kukushkin, D.V. Portnov, A.A. Ivanov, YuI. Belchenko, G.G. Denisov, Tokamak s reaktornymi tekhnologiyami (TRT): kontseptsiya, missii, osnovnyye osobennosti i ozhidayemyye kharakteristiki, Fiz. Plazmy (Moscow) 47 (11) (2021) 970–985, https://doi.org/10.31857/S0367292121110196 (In Russian).

[11] W. Yang, Q. Zeng, C. Chen, Z. Chen, J. Song, Z. Wang, J. Yu, D.V. Yakovlev, V.V. Prikhodko, Shielding design and neutronics calculation of the GDT based fusion neutron source ALIANCE, Fusion Eng. Des. 164 (2021), 112221.

[12] R.W. Moir, N.N. Martovetsky, A.W. Molvik, D. Ryutov, T.C. Simonen, Mirror-based hybrids of recent design, AIP Conf. Proc. 1442 (No. 1) (2012, June) 43–54 (American Institute of Physics).

[13] A.V. Arzhannikov, A.V. Anikeev, A.D. Beklemishev, A.A. Ivanov, I.V. Shamanin, A.N. Dyachenko, O.Y. Dolmatov, Subcritical assembly with thermonuclear neutron source as device for studies of neutron-physical characteristics of thorium fuel. In AIP Conference Proceedings, AIP Publ. LLC 1771 (No. 1) (2016, October), 090004.

[14] Y.E. Titarenko, S.S. Ananyev, V.F. Batyaev, et al., Radiation and nuclear Physics aspects of the use of the thorium fuel cycle in a hybrid fusion facility, Fusion Sci. Technol. 79 (2) (2023) 117–134.

[15] W. Gudowski, V. Arzhanov, C. Broeders, I. Broeders, J. Cetnar, R. Cummings, M. Ericsson, B. Fogelberg, C. Gaudard, A. Koning, P. Landeyro, Review of the European project—impact of Accelerator-Based Technologies on nuclear fission safety (IABAT), Prog. Nucl. Energy 38 (1–2) (2001) 135–151.

[16] J. Knaster, F. Arbeiter, P. Cara, S. Chel, A. Facco, R. Heidinger, A. Ibarra, A. Kasugai, H. Kondo, G. Micciche, K. Ochiai, IFMIF, the European–Japanese efforts under the Broader Approach agreement towards a Li (d, xn) neutron source: current status and future options, Nucl. Mater. Energy 9 (2016) 46–54.

[17] V.V. Prikhodko, A.V. Arzhannikov, Simulations of fusion neutron source based on the axially symmetric mirror trap for the thorium hybrid reactor. In Journal of Physics: conference Series, IOP Publ. 1647 (No. 1) (2020, October), 012004.

[18] I.V. Shamanin, S.V. Bedenko, Y.B. Chertkov, I.M. Gubaydulin, Gas-cooled thorium reactor with fuel block of the Unified design, Izvestiya Wysshikh Uchebnykh Zawedeniy, Yadernaya Energetika 3 (2015) 124–134, https://doi.org/10.26583/npe.2015.3.13 (In Russian).

[19] S.V. Bedenko, N. Ghal-Eh, I.O. Lutsik, I.V. Shamanin, A fuel for generation IV nuclear energy system: isotopic composition and radiation characteristics, Appl. Radiat. Isot. 147 (2019) 189–196.

[20] KSTAR (Korea Superconducting Tokamak Advanced Research). https://www.sciencealert.com/south-korea-s-artificial-sun-just465 set-a-new-world-record-for-high-temperature-plasma. (Accessed 29 November 2021) [online]. South Korea's 'Artificial Sun' Just Set a New World Record for High Temperature Plasma.

[21] EAST (Experimental Advanced Superconducting Tokamak). https://www.scmp.com/news/china/science/article/3161780/chinas-artificial-sun-hits-new-high-clean-energy-boost. (Accessed 3 August 2022) [online]. China's 'artificial sun' hits new high in clean energy boost.

[22] Y.Z. Kandiev, E.A. Kashaeva, K.E. Khatuntsev, E.S. Kuropatenko, L.V. Lobanova, G.N. Lukin, A.A. Malakhov, G.N. Malyshkin, D.G. Modestov, R.F. Mukhamadiev, V.G. Orlov, PRIZMA status, Ann. Nucl. Energy 82 (2015) 116–120.

[23] SERPENT [online]. Serpent 2 Monte Carlo Code version 2.2.0 < https://www.oecd-nea.org/tools/abstract/detail/nea-1923/> (Accessed July 17, 2022).

[24] FloEFD [online]. Siemens Simcenter FloEFD 2021.2.0 v5391 x64 + For NX & Others Free https://tech-story.net/siemens-simcenter-floefd-2021-2-0-v5391-x64-for>. (Accessed June 17, 2022).

[25] J. Gehin, M. Jessee, M.L. Williams, D. Lee, S. Goluoglu, G. Ilas, D. Ilas, S. Bowman, High Temperature Gas-Cooled Reactors, first ed., Elsevier, eBook, 2021 https://doi.org/10.1016/C2018-0-05383-9. (Accessed 27 July 2022).

[26] N. Nojiri, S. Shimakawa, N. Fujimoto, M. Goto, Characteristic test of initial HTTR core, Nucl. Eng. Des. 233 (2004) 283–290.

[27] J. Bess, N. Fujimoto, Benchmark evaluation of start-up and zero-power measurements at the high-temperature engineering test reactor, Nucl. Sci. Eng. 178 (2014) 414–427.

[28] IAEA [online]. International atomic energy agency, Advances in High Temperature Gas Cooled Reactor Fuel Technology, IAEA TECDOC (CD-ROM) No. 1674, IAEA, Vienna, 2013, https://www.iaea.org/publications/10451/advances-in-high-temperature-gas-cooled-reactor-fuel-technology. June 27, 2022).

[29] G. Locatelli, M. Mancini, N. Todeschini, Generation IV nuclear reactors: current status and future prospects, Energy Pol. 61 (2013) 1503–1520.

[30] IAEA [online], International atomic energy agency, IAEA Safeguards Glossary, IAEA, Vienna, Int. Nucl. Verif. Ser. vol. 3 (2003), https://www.iaea.org/publications/6663/iaea-safeguards-glossary. (Accessed 27 July 2022).

[31] H.J. Rütten, K.A. Haas, Research on the incineration of plutonium in a modular HTR using thorium-based fuel, Nucl. Eng. Des. 195 (3) (2000) 353–360.

[32] IAEA [online], Thorium Fuel Cycle – Potential Benefits and Challenges, IAEA-TECDOC-1450 IAEA, Vienna, 2005. https://www.iaea.org/publications/7192/thorium-fuel-cycle-potential-benefits-and-challenges. (Accessed 27 July 2022).

[33] NEA. https://oecd-nea.org/dbdata/data/nds_eval_libs.htm. (Accessed 27 July 2022) [online]. Nuclear Energy Agency, Evaluated Nuclear Data Library Descriptions.

[34] S.V. Bedenko, A.G. Karengin, N. Ghal-Eh, N.I. Alekseev, V.V. Knyshev, I.V. Shamanin, Thermo-physical properties of dispersion nuclear fuel for a new-generation reactors: a computational approach, in: AIP Conference Proceedings vol. 2101, AIP Publishing LLC, 2019, October, 020002. No. 1.

[35] A. Shaimerdenov, S. Gizatulin, D. Dyussambayev, S. Askerbekov, S. Ueta, J. Aihara, T. Shibata, N. Sakaba, Study on the effect of long-term high temperature irradiation on TRISO fuel, Nucl. Eng. Technol. 54 (8) (2022) 2792–2800.